SRI International

Final Report • October 1994

GUEST INVESTIGATOR PROGRAM STUDY: PHYSICS OF EQUATORIAL PLASMA BUBBLES

Roland T. Tsunoda, Principal Scientist
Geoscience and Engineering Center

Contract NAS5-31215
SRI Project 2431

Prepared for:
National Aeronautics and Space Administration
Goddard Space Flight Center
Greenbelt Road
Greenbelt, Maryland 20771

Attention: G. Bullock, Code 602

Approved:

James F. Vickrey, Director
Geoscience and Engineering Center

Murray J. Baron, Vice President
Advanced Development Division

333 Ravenswood Ave • Menlo Park, CA 94025-3493 • (415) 326-6200 • FAX: (415) 326-5512 • Telex: 334486

1 INTRODUCTION

Plasma bubbles are large-scale (10 to 100 km) depletions in plasma density found in the night-time equatorial ionosphere. Their formation has been found to entail the upward transport of plasma over hundreds of kilometers in altitude, suggesting that bubbles play signficant roles in the physics of many of the diverse and unique features found in the low-latitude ionosphere. In the simplest scenario, plasma bubbles appear first as perturbations in the bottomside *F* layer, which is linearly unstable to the gravitationally driven Rayleigh-Taylor instability. Once initiated, bubbles develop upward through the peak of the *F* layer into its topside (sometimes to altitudes in excess of 1000 km), a behavior predicted by the nonlinear form of the same instability. While good general agreement has been found between theory and observations, little is known about the detailed physics associated with plasma bubbles.

Our approach in this research program was to combine two-dimensional bubble characterization (in an overview sense) from backscatter maps obtained with ALTAIR (a steerable incoherent-scatter radar) with high-resolution but one-dimensional measurements obtained with *in situ* sensors onboard the Atmosphereic Explorer-E (AE-E) and San Marco D (SM-D) satellites. Both of these satellites were in low-inclination, low-altitude orbits that allowed *in situ* measurements during traversals of plasma bubbles in directions that are nearly aligned with planes transverse to the geomagnetic field and the east-west regions scanned by ALTAIR. High-resolution *in situ* measurements could be used to examine the microphysics associated with irregularity production and dynamics and could be viewed in perspective by comparing them to sequences of ALTAIR backscatter maps that could provide the time evolution of plasma bubbles. In addition, we used other ground-based measurements made during overpasses of the satellites to provide continuous measurements of bubble activity.

2 SUMMARY OF RESULTS

Our research activity centered around two topics: the shape of plasma bubbles and associated electric fields, and the day-to-day variability in the occurrence of plasma bubbles. The first topic was pursued because of a divergence in view regarding the nonlinear physics associated with plasma bubble development. While the development

of perturbations in isodensity contours in the bottomside *F* layer into plasma bubbles is well accepted, some believed bubbles to be cylinder-like closed regions of depleted plasma density that floated upward leaving a turbulent wake behind them [e.g., Woodman and LaHoz, 1976; Ott, 1978; Kelley and Ott, 1978]. Others believed the bubbles to be more wedgelike and vertically elongated [e.g., Scannapieco and Ossakow, 1976; Tsunoda et al., 1982]. These different perceptions about the geometry of bubbles led to different conclusions regarding the electrodynamics of plasma bubbles. For example, the observations of bubbles with supersonic speeds [e.g., Aggson et al., 1992] have led to consideration of more exotic source mechanisms. Our results, summarized in a paper submitted to the *Journal of Geophysical Research* [Tsunoda et al., 1994], consisted of incoherent scatter radar measurements that showed unambiguously that the depleted region is wedgelike and not cylinderlike, and a case study and modeling of SM-D electric field instrument (EFI) measurements that showed that the absence of electric-field perturbations outside the plasma-depleted region is a distinct signature of wedge-shaped plasma bubbles. The existence of wedgelike bubbles also simplifies the interpretation of supersonic bubbles in terms of the ordinary flux-tube-interchange process associated with the Rayleigh-Taylor instability.

The second topic was pursued because the inability to predict the day-to-day occurrence of plasma bubbles indicated inadequate knowledge of the physics of plasma bubbles. An understanding of bubble formation requires an understanding of the roles of the various terms in the linearized growth rate of the collisional Rayleigh-Taylor instability. In addition, consideration has to be given to the sources and amplitudes of seed perturbations that are amplified by the instability into plasma bubbles. Most of the attention has been given to the growth-rate terms [e.g., Maruyama and Matuura, 1984; Tsunoda, 1985; Mendillo et al., 1992] and the possiblity of seeding bubbles *in situ* in the *F* region [e.g., Kelley et al., 1981; Anderson et al., 1982; Hysell et al., 1990]. In our study, we examined electric-field perturbations found in SM-D EFI data and found that the seeding is more likely to be produced in the *E* region rather than the *F* region. The results of this investigation are presented in the Appendix of this report and will be submitted for publication in the *Journal of Geophysical Research.*

3 REFERENCES

Aggson, T.L., W.J. Burke, N.C. Maynard, W.B. Hanson, P.C. Anderson, J.A. Slavin, W.R. Hoegy, and J.L. Saba, Equatorial bubbles updrafting at supersonic speeds, *J. Geophys. Res.*, *97*, 8581, 1992.

Anderson, D.N., A.D. Richmond, B.B. Balsley, R.G. Roble, M.A. Biondi, and D.P. Sipler, In-situ generated gravity waves as a possible seeding mechanism for equatorial spread *F*, *Geophys. Res. Lett.*, 9, 789, 1982.

Hysell, D.L., M.C. Kelley, W.E. Swartz, and R.F. Woodman, Seeding and layering of equatorial spread *F* by gravity waves, *J. Geophys. Res.*, *95*, 17,253, 1990.

Kelley, M.C., and E. Ott, Two-dimensional turbulence in equatorial spread *F*, *J. Geophys. Res.*, *83*, 4369, 1978.

Kelley, M. C., M. F. Larsen, C. LaHoz, and J. P. McClure, Gravity wave initiation of equatorial spread *F*: a case study, *J. Geophys. Res.*, *86*, 9087, 1981.

Maruyama, T., and N. Matuura, Longitudinal variability of annual changes in activity of equatorial spread *F* and plasma bubbles, *J. Geophys. Res. 89*, 10,903, 1984.

Mendillo, M., J. Baumgardner, X. Pi, P. J. Sultan, and R. Tsunoda, Onset conditions for equatorial spread *F*, *J. Geophys. Res.*, *97*, 13,865, 1992.

Ott, E., Theory of Rayleigh-Taylor bubbles in the equatorial ionosphere, *J. Geophys. Res.*, *83*, 2066, 1978.

Scannapieco, A.J., and S.L. Ossakow, Nonlinear equatorial spread *F*, *Geophys. Res. Lett.*, *3*, 451, 1976.

Tsunoda, R. T., Control of the seasonal and longitudinal occurrence of equatorial scintillations by the longitudinal gradient in integrated *E* region Pedersen conductivity, *J. Geophys. Res.*, *90*, 447, 1985.

Tsunoda, R.T., R.C. Livingston, J.P. McClure, and W.B. Hanson, Equatorial plasma bubbles: Vertically elongated wedges from the bottomside *F* layer, *J. Geophys. Res.*, *87*, 9171, 1982.

Tsunoda, R.T., T.L. Aggson, and W.B. Hanson, On the geometric shape of equatorial plasma bubbles and associated polarization electric fields, submitted to *J. Geophys. Res.*, 1994.

Woodman, R.F., and C. LaHoz, Radar observations of *F*-region equatorial irregularities, *J. Geophys. Res.*, *81*, 5447, 1976.

APPENDIX

ON THE SEEDING OF PLASMA BUBBLES BY LARGE-SCALE WAVES IN THE EQUATORIAL IONOSPHERE

By

Roland T. Tsunoda
Geoscience and Engineering Center
SRI International
Menlo Park, California

William B. Hanson
Center for Space Science
University of Texas at Dallas
Richardson, Texas

Thomas L. Aggson
National Aeronautics and Space Administration
Goddard Space Flight Center
Greenbelt, Maryland

To be submitted to the
Journal of Geophysical Research

ABSTRACT

We examine the role of seeding in the day-to-day variability of equatorial spread-F occurrence. Using electric field ($\vec{E}$)and ion density measurements made from the San Marco-D satellite in conjunction with ground-based measurements from the Kwajalein Atoll, Marshall Islands, we show that $\vec{E}$ perturbations that occur in the pre-sunset period play a role in the development of plasma bubbles. Perturbations in the eastward electric-field component with amplitudes as large as 0.9 mV/m (i.e., 30 m/s upward) were found to exist in the absence of corresponding perturbations in the vertical electric-field component or in plasma density. We interpret these results as indicating that the dynamo source of the perturbation electric field was not located where the measurements were made. This observation, combined with the fact that these perturbations can occur prior to E-region sunset, is consistent with the hypothesis that the perturbations develop in the E region and are mapped up to the F layer, a dynamo scenario that would be more effective under sunlit conditions. We further show that these $\vec{E}$ perturbations can occur under both quiet and active magnetic conditions.

1 INTRODUCTION

Considerable progress has been made in understanding the processes responsible for plasma structure in the night-time equatorial *F* layer, known categorically as equatorial spread *F* (ESF). There is general agreement that the primary source of plasma structure (with spatial scales greater than the ion gyroradius) is the gravity-driven, magnetic flux-tube interchange instability, i.e., the Rayleigh-Taylor instability [*Dungey*, 1956; *Balsley et al.*, 1972; *Haerendel*, 1973]. Near-consensus agreement was reached when plasma structure found in the topside *F* layer [e.g., *Hanson and Sanatani*, 1973; *Woodman and LaHoz*, 1976] could be accounted for by the nonlinear form of the collisional Rayleigh-Taylor (CRT) instability [*Scannapieco and Ossakow*, 1976]. While roles are being played by drivers other than gravity and by other instability processes to produce the observed electrodynamics and plasma-structure characteristics, the CRT instability clearly plays the lead role in the generation of ESF.

That ESF is controlled by the CRT instability is indicated by the fact that the seasonal and longitudinal occurrence of ESF are accountable in terms of the various terms in the growth rate expression for the CRT instability. For example, *Maruyama and Matuura* [1984] suggested that a transequatorial neutral wind would weaken the growth rate of the CRT instability by producing a hemispherical asymmetry in *F*-region plasma-density distribution. *Tsunoda* [1985], on the other hand, suggested that the growth rate is enhanced in situations where the solar terminator is aligned with the conjugate *E* regions; this alignment is believed to lead to the development of a stronger eastward electric field during the post-sunset rise of the *F* layer. While all features found in the seasonal and longitudinal morphology of ESF have not been accounted for, the results described in the above two references have lent confidence to current beliefs.

On the other hand, the day-to-day variability in the occurrence of ESF continues to elude predictive description. The problem is that the easily measurable parameters that can be related to the growth rate of the CRT instability do not, by themselves, exert clear control. For example, there have been numerous investigations into the dependence of ESF occurrence on the altitude of the *F* layer or the rate of increase in that altitude [e.g., *Farley et al.*, 1970]. While both contribute to the statistical behavior of ESF occurrence, neither appear to control the day-to-day variability. *Mendillo et al.* [1992] conducted a two-night case study and found that ESF development was weaker when the latitudinal gradient in 630.0 nm airglow was also weaker. They showed through some modeling

that this observed behavior could be produced by such a wind, and suggested that the day-to-day variability in ESF occurrence may reflect a variability similar to that of the transequatorial wind. The mechanism is the same as that suggested by *Maruyama and Matuura* [1984]; only the variability is thought to occur on shorter time scales. More recently, *Raghavarao et al.* [1988] have reported that there is high correlation between the development of the equatorial (Appleton) anomaly in the afternoon and the subsequent night-time development of ESF. Why the equatorial anomaly develops in the afternoon and how it acts to control the occurrence of ESF remains to be addressed.

Seeding is also a possible source of the day-to-day variability. All indications are that the growth rate of the CRT instability is too small to amplify thermal plasma fluctuations into the observed plasma structure. For this reason, a nonthermal perturbation in plasma density is needed so that it can be amplified into the observed plasma structure. *Röttger* [1973] was the first to consider atmospheric gravity waves (AGW) as the source controlling the quasi-periodic occurrence in space and time of large-scale upwellings in the bottomside *F* layer. A number of other investigations have been conducted to consider the extent to which AGWs can produce wave structure in plasma density [*Klostermeyer*, 1978; *Kelley et al.*, 1981; *Tsunoda and White*, 1981; *Hysell et al.*, 1990]. If seeding by AGWs is the controlling source of the day-to-day variability in ESF occurrence, the variability would then come from that associated with AGW activity.

In this paper, we consider the question of seeding using electric-field ($\vec{E}$) measurements made by the San Marco D (SM-D) satellite, and related measurements made by an AFSATCOM scintillation receiver, ALTAIR incoherent-scatter radar, and a frequency-agile radar (FAR). (The importance of the $\vec{E}$ measurements is that they represent true plasma motion and not apparent motions associated with isodensity surfaces.) The ground measurements were made as part of the 1988 PEAK program sponsored by the Defense Nuclear Agency and as part of the 1992 NICE program sponsored by the National Science Foundation.

2 WAVELIKE STRUCTURES: EARLIER RESULTS

The existence of large-scale wavelike structures in the bottomside of the nighttime equatorial *F* layer was first reported by *Röttger* [1973]. He found, from transequatorially propagated radio signals, that the spatial scales of these structures in the east-west direction were distributed between 210 and 640 km (lower and upper quartile values) with a median value of 380 km. *Tsunoda and White* [1981] confirmed that these structures could, in fact, be quasi-sinusoidal when described by isodensity contours. They used incoherent-scatter (IS) measurements made with the ALTAIR radar [e.g., *Tsunoda et al.*, 1979] to show that the spatial separations of the upwellings in their case study were about 400 km, similar to the median value obtained by *Röttger* [1973]. They further showed that these large-scale altitude modulations of the bottomside *F* layer did indeed lead to the development of plasma bubbles (and radar backscatter plumes) from the crests of the upwellings. This pattern of a quasi-periodic seed perturbation leading to the development of plasma bubbles is consistent with the results from nonlinear computer simulations of the CRT instability [*Scannapieco and Ossakow*, 1976; *Zalesak et al.*, 1982].

Because the descriptors of these quasi-periodic patterns resemble medium-scale, traveling ionospheric disturbances, *Röttger* [1973] suggested that they were produced by interaction with AGW. To account for the large amplitudes of these undulations, he suggested that spatial resonance [*Whitehead*, 1971] could act to produce the altitude modulation of isodensity contours. The concept of spatial resonance was pursued theoretically and experimentally by others [e.g., *Klostermeyer*, 1978; *Kelley et al.*, 1981]. The problem with direct amplification by AGWs, however, is that the growth rate cannot exceed the wind amplitude of the AGW [e.g., *Tsunoda and White*, 1981; *Kelley et al.*, 1981]. On the other hand, AGW interaction with *F*-region plasma could still control the seeding process and, thus, the day-to-day variability of ESF occurrence.

The preferential occurrence of large-scale plasma structures with spatial wavelengths on the order of several hundred kilometers must contain key information regarding the source of the seeding process. This question has been addressed by several researchers. *Anderson et al.* [1982] suggested that an instability in the neutral-wind shear could be responsible for in situ amplification of the longer scale perturbations. *Guzdar et al.* [1982] suggested that a shear in plasma flow modifies the CRT instability and produces a maximum in growth rate at a longer spatial scale size. A difficulty with this

latter proposition is that the growth rate at the preferred scale size is much weaker than that for smaller spatial scales in the absence of a velocity shear.

Hysell et al. [1990] described the presence of sloping streaks in Jicamarca radar backscatter data, which they interpreted as the first evidence of layering. They associated the layering with the vertical wavelength (about 50 km) of the instigating AGW. They argued from their case study that this is convincing evidence that AGWs are the primary seeding source for ESF. This event occurred during a magnetically disturbed period (Kp index was 6– during the sunset period); the giant backscatter plumes that occurred on that night were thought to be a consequence of direct penetration of the magnetospheric $\vec{E}$, which enhanced upward plasma drift. The spacings (20 to 40 min) of the three backscatter plumes were attributed to some sort of interaction with a zonally propagating AGW. A difficulty with this proposition is that they depend on $M > 1$ (i.e., a partially conducting E layer) to drive a vertical current and cause layering by the CRT instability. The growth rate, therefore, must always be less than that for the insulated F layer case.

Earle and Kelley [1987] investigated the frequency dependence of the penetration of $\vec{E}$ from the magnetosphere to the equatorial ionosphere, in the range from 1 to 10 hr. They conducted a spectral analysis of $\vec{E}$ measured by the various IS radars. They asserted that there are two main sources: AGWs during quiet times and magnetospheric $\vec{E}$ during disturbed times. Magnetospheric $\vec{E}$, for periods less than 10 hr easily penetrates to the equator. The authors present a data set of Chatanika, Arecibo, and Jicamarca IS measurements that show the $L^{3/2}$ dependence predicted by geometric projection [*Mozer*, 1970]. For fluctuation periods less than 5 hr, the magnetospheric source dominates for Kp $\geq$ 3 at Jicamarca. Interestingly, these researchers analyzed only 24-hr continuous runs at Jicamarca that did not contain ESF.

Nair et al. [1992] operated a 5.5 MHz Doppler radar and measured vertical-drift fluctuations and their spectra during the post-sunset period. The fluctuation spectra contained components from a few minutes to several tens of minutes. The dominant period of the fluctuations was a few tens of minutes, while the most frequent was around 30 min. The periods showed no dependence on magnetic activity. The measurements show that the amplitude of the fluctuations is amplified during the post-sunset rise of the F layer and attains its maximum value around the time of the reversal in vertical velocity. The amplitude of the fluctuations ranged from less than 1 m/s to about 15 m/s. The maximum perturbation amplitudes seen on moderately disturbed nights were smaller than those found on quiet or highly disturbed nights. (This dependence, however, was not clear in the amplitudes prior to or after the velocity reversal.) There is a problem with

using high-frequency reflected signals to determine the EW electric-field perturbations. Once wavelike isodensity contours form, their horizontal drift will appear to produce oscillatory, apparent, vertical motions; these Doppler variations would not be true vertical plasma motions except in cases where the amplitude of the altitude modulation is small. Their maximum amplitudes of 15 m/s, however, are comparable to the San Marco $\vec{E}$ perturbations presented in this paper.

The issues regarding seeding have to do with their source mechanism: that is, is the source in the bottomside *F* layer, as presumed by most researchers, or elsewhere; and are the observed amplitudes of the wavelike structures produced by the seed mechanism or by another amplification or damping process? *Tsunoda and White* [1981] have presented evidence that wave structure seen in the bottomside *F* layer is of significant amplitude even at the time of *E*-region sunset. For this reason, they concluded that the altitude modulation seen in the *F* layer is likely produced by the *E*-region dynamo prior to *E*-region sunset. Another issue has to do with the anticorrelation of ESF occurrence with magnetic activity. Is the amplitude of the seed affected by magnetic activity, as suggested implicitly by *Earle and Kelley* [1987] when they attributed $\vec{E}$ perturbations to AGWs during low magnetic activity and to the penetration of the magnetospheric $\vec{E}$ during high magnetic activity?

3 RESULTS

3.1 San Marco-D Electric-Field Measurements

The San Marco D (SM-D) satellite was launched on 25 March 1988 into a low-inclination (2.9°) orbit with an apogee of 610 km and an perigee of 275 km. Two of the instruments on board were the electric field instrument (EFI) and the ion drift meter (IDM). Their combined measurements make it possible to determine the spatial relationship between plasma density and electric field. The EFI and some of the first results were presented by *Aggson et al.* [1992]. Data collected in the Kwajalein sector during August 1988 were used to provide a sampling of the seeds that were present. In the following, we describe three examples of $\vec{E}$ perturbations seen in the EFI data. We then tabulate the seeding events and summarize their characteristics.

The first example of $\vec{E}$ perturbations was taken on 1 August 1988 (Day 214). Electric field measurements were first made during a pass over the Kwajalein sector between 0626:58 and 0629:18 UT. Those contained no evidence of $\vec{E}$ perturbations. Prominent perturbations were seen, however, in the measurements taken during the next pass over the same longitude sector between 0804:35 and 0807:55 UT. The eastward component of $\vec{E}$ is shown plotted as a function of universal time in the top panel of Figure 1. The tick marks are shown at 20 s intervals. A smooth dashed curve has been drawn to show the perturbations more clearly. (The negative slope is believed to reflect the initial corrections from the attitude control when the satellite instruments were first turned on.) We see that the perturbations, as displayed, are eastward with the largest pertubation occurring around 0805:25 UT at a longitude to the west of Kwajalein. The location of Kwajalein is marked by the downward pointing arrow along the abscissas. The variation of interest that occurred over a 40 s period corresponds to an east-west (EW) distance of about 280 km. (The rather regular, finer scale structure is instrumental and should be ignored.) The amplitude of the perturbation (referenced to the dashed curve) is estimated to be about 0.9 mV/m, which corresponds to a plasma drift of about 30 m/s for a geomagnetic field strength of 0.3 G. We see that this perturbation in $\vec{E}$ is followed by another smaller perturbation to the east and a plasma bubble beyond that second perturbation. (A portion of a second plasma bubble can be seen near the right edge of the plot.) The spacings of the perturbations and the bubble are roughtly equal, about 300 km apart, suggesting that the bubble was perhaps related to the $\vec{E}$ perturbations. The eastward $\vec{E}$ component within the bubble was as large as 8 mV/m,

which corresponds to 160 m/s, a typical updrafting velocity [e.g., *Hanson and Bamgboye*, 1984]. Except for a depletion in plasma density associated with the plasma bubbles, there were no other perturbations in plasma density. Without any perturbations discernible in the vertical $\vec{E}$ component, this signature appears as a seed perturbation in $\vec{E}$ and not in plasma density.

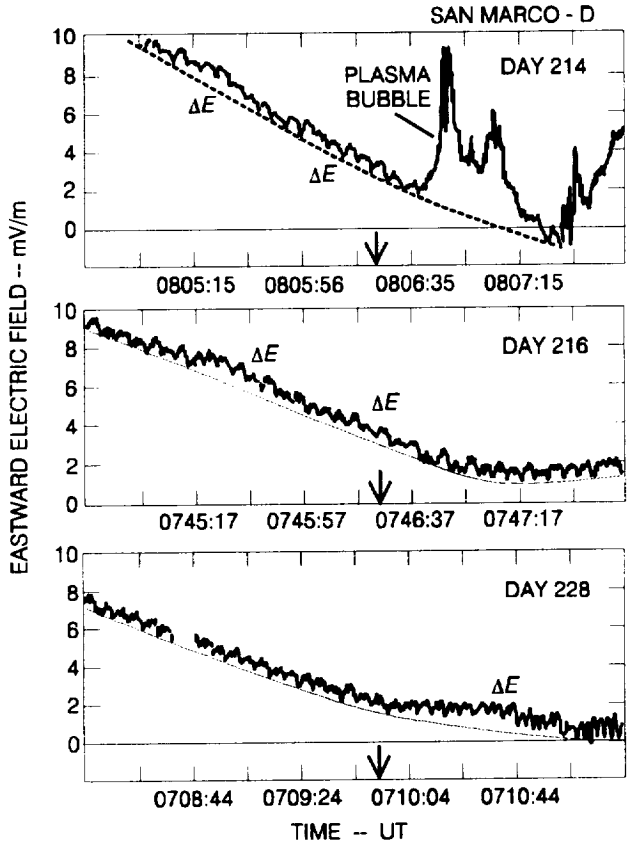

Figure 1. Examples of $\vec{E}$ perturbations in San Marco-D satellite data.

The second example, taken on 3 August 1988 (Day 216), is shown in the center panel of Figure 1. In this example, which occurred around 0746 UT in the Kwajalein sector, the $\vec{E}$ perturbations are similar to those in the top panel, both in amplitude and spatial scale. While plasma bubbles were not seen to the east of these perturbations, strong scintillations measured from Kwajalein were found to commence around 0830 UT. As in the first example, the perturbations were only in the eastward $\vec{E}$ component and not in plasma density. We note that the perturbation occurred about 20 min earlier in local time than that in the top panel. In comparison, the earliest scan made by *Tsunoda and White* [1981] from 0743 to 0803:20 UT, contained wavelike variations in plasma

density. Those were seen at times when the solar zenith angle was 104° at the east end of the scan and 98° at the west end.

The third example was taken on 15 August 1988 (Day 228), during a pass over the Kwajalein sector at an even earlier time. In this case, we can see a single $\vec{E}$ perturbation that is somewhat larger in amplitude than those in the two upper panels and which occurred to the east of Kwajalein around 0710:34 UT. Again, perturbations could not be found in either the vertical $\vec{E}$ component or in plasma density. Strong scintillations were found to commence abruptly around 0820 UT.

To gain perspective, we have listed (Table 1) the occurrences of seed perturbations in EFI data taken during San Marco passes over the Kwajalein sector in August during the ±1.5 hour period centered on *E*-region sunset. We have listed the times of occurrence of $\vec{E}$ perturbations, whether ESF followed in the 0800 to 0900 UT (1910 to 2010 LST time period), the Kp indices for this period, and the sum of the Kp indices for those days. The ESF conditions were determined from the AFSATCOM scintillation measurements, which were also made from Kwajalein throughout August. Scintillation is a useful measure of ESF because it is produced primarily by kilometer-scale irregularities that persist once they are produced. This means that the detection of scintillation indicates the onset of structure development to the west of the Kwajalein longitude and at some time prior to the observations.

Scanning through the list of EFI data, we find that seed perturbations were detected in the San Marco $\vec{E}$ measurements at times as early as 0626:17 UT in the Kwajalein sector, although that event did not lead to ESF development. Another perturbation, detected at 0643:22 UT, was followed by ESF development. Both perturbations, although weaker in strength than those in Figure 1, occurred well before *E*-region sunset. Examples of this kind lend support to the hypothesis that the *E*-region dynamo could be more efficiente than the *F*-region dynamo as a seed sourc.

To summarize our findings from Table 1, we have plotted (Figure 2) a histogram for the occurrences of seeds and an inverted histogram for passes that did not contain seeds, both as a function of the magnetic Kp index. Out of 32 SM-D satellite passes over Kwajalein, 12 contained seeds while 20 did not contain seeds (i.e., seeds were observed 60% of the time). In comparison, ESF activity was observed in the 0800 to 0900 UT period on 13 out of 29 passesr (45% of the time). We, therefore, find that the percentage occurrences of seeds and ESF activity were comparable. The seeded and nonseeded events are also distributed between Kp values of 0 and 5 with broad maxima in both

between 1 and 3. Because of the similarities in distribution, we cannot conclude that the seeding events show any obvious Kp dependence. We can say, however, that seeds can occur under relatively quiet magnetic-activity conditions. On the other hand, the absence of perturbations during periods of higher magnetic activity does suggest that most of the observed perturbations are not of magnetospheric origin.

Table 1
Seeding Events in August 1988

Day	DOY	Pass Time (UT)	H_S (km)	Seed Time (UT)	ESF (8-9)	Kp	ΣKp
1	214	0626:58	355	N	--	3-/2+	15
1	214	0804:35	413	0805:25	--	3-/2+	15
2	215	0705:22	361	N	--	2/1	11+
3	216	0744:37	366	**0745:27**	**0830**	3-/**2+**	**13-**
4	217	0645:07	318	N	N	1/0+	4
4	217	0823:38	371	0824:37	N	1/0+	4
5	218	0723:56	322	0726:16	N	1/1+	12+
6	219	0624:07	282	0626:17	N	2-/3-	11-
7	220	0702:32	286	N	N	1+/1	10
8	221	0740:45	289	**0741:45**	**0830**	0+/**1-**	**6-**
10	223	0718:18	263	N	N	1+/1+	16-
11	224	0755:57	265	0757:17	N	2-/2	17
12	225	0655:08	251	N	0838	2+/2+	24-
13	226	0732:23	251	N	N	4-/3-	26-
15	228	0708:04	253	**0710:34**	**0820**	3+/**4+**	**24**
17	230	0643:05	271	N	N	2/2-	10-
18	231	0719:25	269	**0720:58**	**0810**	3+/**2**	**17-**
19	232	0617:21	303	N	0830	2/2-	16+
20	233	0653:23	300	N	N	3-/3-	24-
21	234	0729:16	303	N	0845	2/2-	12+
22	235	0626:46	341	N	N	6/4-	23+
23	236	0702:20	338	N	0820	2/2+	19+
24	237	0559:26	388	N	N	2/2-	19+
26	239	0709:47	381	**0711:37**	**0840**	3-/**2-**	17
27	240	0606:19	429	N	N	4-/3	23
27	240	0744:42	377	N	N	4-/3	23
28	241	0641:02	426	**0643:22**	**0840**	2/**2+**	**17+**
29	242	0537:07	467	N	N	2+/4-	21+
29	242	0715:34	422	N	N	2+/4-	21+
30	243	0611:27	464	N	0900	3+/4	21-
30	243	0749:53	419	**0752:20**	**0900**	3+/**4**	**21-**
31	244	0507:06	491	N	0830	2/1	20-

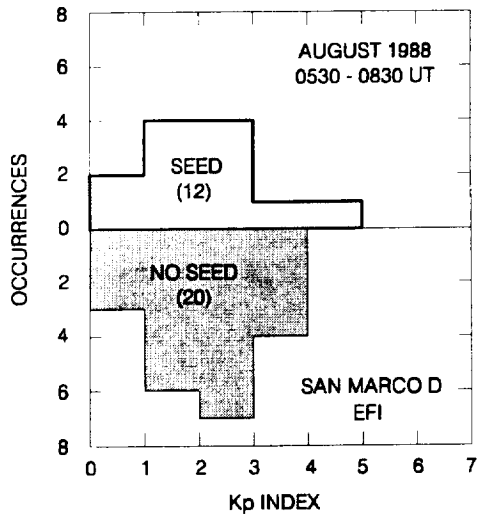

Figure 2. Histograms showing the occurrences and non-occurrences of seed $\vec{E}$ perturbations on any given San Marco satellite pass through the Kwajalein sector in the time interval 0530 to 0830 UT.

To test the relationship between the detection of a seed perturbation in $\vec{E}$ and the subsequent development of ESF, we tabulated (Table 2) the number of passes in which a seed was detected and whether or not ESF followed. We see from the numbers that there is a tendency for seeds to be followed by the development of ESF. That is, the number of occurrences when seeds were followed by ESF development is almost twice as many as that when seeds were detected but not followed by ESF development. Similarly, the number of occurrences when both seeds and ESF were absent is almost twice as many as that when seeds were not detected but were followed by ESF development. But when we applied Fisher's test for statistical significance, we found that this apparent correlation was below the accepted level for claiming a definite relationship. We, therefore, conclude that while there may exist a causal relationship, it is not very strong.

Table 2
Seed/ESF Relationship

	ESF	No ESF
Seed	7	4
No Seed	5	9

3.2 Wave Structure Under Disturbed Conditions

Although the San Marco EFI measurements during August 1988 did not contain seeding events that occurred during magnetically disturbed conditions, we have radar evidence of wave structure that developed under such conditions. The SRI FAR

[*Tsunoda et al.*, 1994] was operated as an unattended ionosonde (except for data media changes) from the Kwajalein Atoll, Marshall Islands for two weeks in August 1992. Data from the late afternoon through the pre-midnight sector on 5 August 1992 were found to contain features that can be related to $\vec{E}$ perturbations of the kind described above.

The wavelike features of interest are seen in Figure 3 where we have plotted the virtual height of *F*-region reflections as a function of time for an operating frequency of 5.54 MHz. The 7-hour period, shown from 0500 to 1200 UT, corresponds with local solar times from 1610 to 2310 LST. The magnetic Kp indices were 6–, 5, and 4 during this period, indicating high but declining magnetic activity. We see a sporadic *E* layer around 100-km altitude, the first, and second-hop *F* traces, and other mixed reflection modes, the last occurring at times prior to 0700 UT. The post-sunset rise of the *F* layer is evident from the first-hop *F* trace beginning shortly after 0700 UT and lasting until about 0815 UT. Range spread echoes commenced around 0820 UT and persisted for the remainder of the period as the *F* layer descended. (The *F* trace between 0500 and 0800 UT is discrete, indicating a smooth *F* layer. The trace appears diffuse because of the presence of range sidelobes generated by the 7-baud Barker-coded waveform that was used by the FAR.)

Wavelike oscillations in the *F* trace are seen prior to the post-sunset rise of the *F* layer, appearing as early as 0600 UT and continuing until 0700 UT. These oscillations are seen more clearly in the second-hop *F* trace; we can discern about 1-1/2 cycles over an approximate period of 40 min. The oscillations appear to continue during the rise of the *F* layer, although, there are less clear than in preceding hours. And, interestingly, these wavelike variations are similar to the variations in virtual height of the leading edge of the range spread echoes that follow thereafter. Although difficult to estimate, the nominal period seems to be around 45 min. All of these oscillations could be represented by 6 cycles in a single corrugated structure that had a period that varied from 40 to 48 min. These periods are similar to those estimated by *Röttger* [1973] and *Hysell et al.* [1990]. If we assume an eastward drift of 100 m/s, a 40-min period corresponds to a spatial wavelength of 240 km. These oscillations, therefore, are similar to the wave structure reported by *Tsunoda and White* [1981].

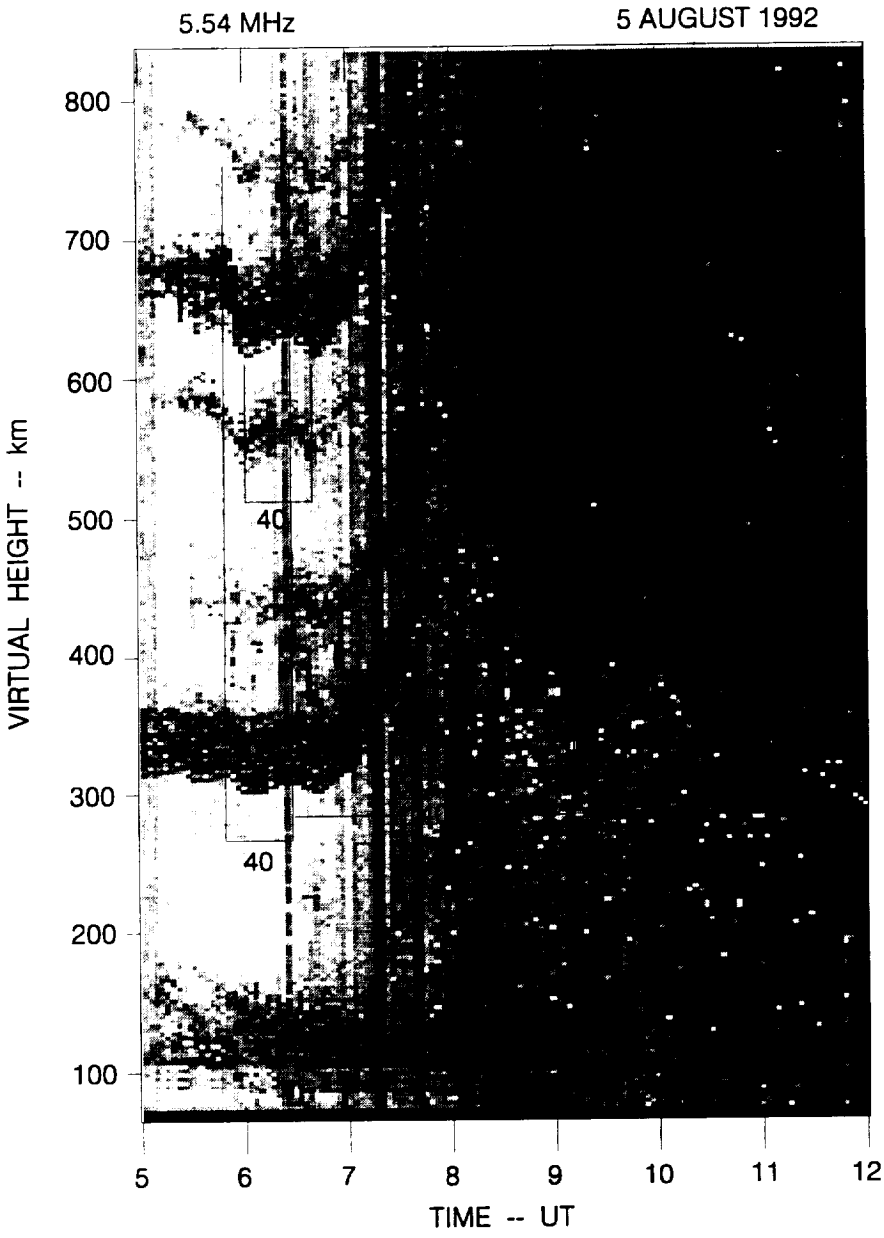

Figure 3. Example of wave structure that occurred prior to the post-sunset rise of the *F* layer under magnetically disturbed conditions.

Other than the fact that wavelike oscillations were observed during a period of high magnetic activity, it is interesting to note that they appeared to commence more than an hour before *E*-region sunset, which occurs at the beginning of the post-sunset rise of the *F* layer. The onset of these wavelike variations occurs more than 30 min earlier than the earliest seed event discussed above. We, therefore, can state conclusively that the wave structure developed under sunlit conditions.

4 DISCUSSION AND CONCLUSIONS

We found that $\vec{E}$ perturbations occur in the equatorial ionosphere at times prior to as well as after E-region sunset. The perturbations were found only in the eastward component and not in the vertical component, with $\vec{E}$ perturbation as large as 0.9 mV/m, or about 30 m/s. The $\vec{E}$ perturbations found in San Marco data appear to be of the same scale sizes as those reported by *Röttger* [1973]. The EW dimension and spacings are on the order of several hundred kilometers, which are also similar to the wave structure reported by *Tsunoda and White* [1981]. In virtually all cases, the perturbations were not accompanied by perturbations in plasma density. In this sense, we consider these $\vec{E}$ perturbations to be seeds that could lead to the development of plasma bubbles. The significance of these observations is that if a wave structure is produced under sunlit conditions, its source is unlikely to be interactions with an AGW in the F region. The so-called gravity-wave dynamo would not be as effective under these conditions, for the same reasons the F-region dynamo is not operative under sunlit conditions. These reults, therefore, suggest that if the wave structure is a result of a gravity-wave dynamo, it must have occurred in the E region.

Quasi-periodic echoes have been observed in the mid-latitude E region in the evening sector [e.g., *Fukao et al.*, 1991; *Yamamoto et al.*, 1991]. *Tsunoda et al.* [1994] suggested that an altitude-modulated sporadic E (E_s) layer could set up polarization electric fields. If E_s layer move toward the equatorial regions, there is reason to expect their effects at lower latitudes. Whether such phenomena could be associated with seeding remains to be investigated. We need to consider the geometry for a southwest propagating sheet of E_s and its intersection with bottomside F-layer field lines.

REFERENCES

Aggson, T.L., N.C. Maynard, W.B. Hanson, and J.L. Saba, Electric field observations of equatorial bubbles, *J. Geophys. Res.*, *97*, 2997, 1992.

Anderson, D.N., A.D. Richmond, B.B. Balsley, R.G. Roble, M.A. Biondi, and D.P. Sipler, In-situ generated gravity waves as a possible seeding mechanism for equatorial spread *F*, *Geophys. Res. Lett.*, 9, 789, 1982.

Balsley, B.B., G. Haerendel, and R.A. Greenwald, Equatorial spread *F*: Recent observations and a new interpretation, *J. Geophys. Res.*, *77*, 5625, 1972.

Dungey, J.W., Convective diffusion in the equatorial *F* region, *J. Atmos. Terr. Phys.*, *9*, 304, 1956.

Earle, G.D., and M.C. Kelley, Spectral studies of the sources of ionospheric electric fields, *J. Geophys. Res.*, *92*, 213, 1987.

Farley, D.T., B.B. Balsley, R.F. Woodman, and J.P. McClure, Equatorial spread *F*: implications of VHF radar observations, *J. Geophys. Res.*, *75*, 7199, 1970.

Fukao, S., M.C. Kelley, T. Shirakawa, T. Takami, M. Yamamoto, T. Tsuda, and S. Kato, Turbulent upwelling of the mid-latitude ionosphere: 1. Observational results by the MU radar, *J. Geophys. Res.*, *96*, 3725, 1991

Guzdar, P.N., P. Satyanarayana, J.D. Huba, and S.L. Ossakow, Influence of velocity shear on the Rayleigh-Taylor instability, *Geophys. Res. Lett.*, *9*, 547, 1982

Haerendel, G., Theory of equatorial spread *F*, preprint, Max-Planck-Institut für Physik und Astrophysik, Institut für extraterrestrische Physik, Garching, FRG, 1973.

Hanson, W.B., and D.K. Bamgboye, The measured motions inside equatorial plasma bubbles, *J. Geophys. Res.*, *89*, 8997, 1984.

Hanson, W.B., and S. Sanatani, Large N_i gradients below the equatorial *F* peak, *J. Geophys. Res.*, *78*, 1167, 1973.

Hysell, D.L., M.C. Kelley, W.E. Swartz, and R.F. Woodman, Seeding and layering of equatorial spread *F* by gravity waves, *J. Geophys. Res.*, *95*, 17,253, 1990.

Kelley, M.C., M.F. Larsen, and C. LaHoz, Gravity wave interaction of equatorial spread *F*: a case study, *J. Geophys. Res.*, *86*, 9087, 1981.

Klostermeyer, J., Nonlinear investigation of the spatial resonance effect in the nighttime equatorial *F* region, *J. Geophys. Res.*, *83*, 3753, 1978.

Maruyama, T., and N. Matuura, Longitudinal variability of annual changes in activity of equatorial spread *F* and plasma bubbles, *J. Geophys. Res.*, *89*, 10,903, 1984.

Mendillo, M., J. Baumgardner, X. Pi, P.J. Sultan, and R. Tsunoda, Onset conditions for equatorial spread *F*, *J. Geophys. Res.*, *97*, 13,865, 1992.

Mozer, F.S., Electric field mapping in the ionosphere at the equatorial plane, *Planet. Space Sci.*, *18*, 259, 1970.

Nair, R.B., N. Balan, G.J. Bailey, and P.B. Rao, Spectra of the ac electric fields in the post-sunset *F* region at the magnetic equator, *Planet. Space Sci.*, *40*, 655, 1992.

Raghavarao, R., M. Nageswararao, J.H. Sastri, G.D. Vyas, and M. Sriramarao, Role of equatorial ionization anomaly in the initiation of equatorial spread *F*, *J. Geophys. Res.*, *93*, 5959, 1988.

Röttger, J., Wavelike structures of large scale equatorial spread F irregularities, *J. Atmos. Terr. Phys.*, *35*, 1195, 1973.

Scannapieco, A.J., and S.L. Ossakow, Nonlinear equatorial spread *F*, *Geophys. Res. Lett.*, *3*, 451, 1976.

Tsunoda, R.T., Control of the longitudinal and seasonal occurrence of equatorial scintillations by the longitudinal gradient in integrated *E*-region Pedersen conductivity, *J. Geophys. Res.*, *90*, 447, 1985.

Tsunoda, R.T., and B.R. White, On the generation and growth of equatorial backscatter plumes, 1. Wave structure in the bottomside *F* layer, *J. Geophys. Res.*, *86*, 3610, 1981.

Tsunoda, R.T., M.J. Baron, J. Owen, and D.M. Towle, Altair: an incoherent scatter radar for equatorial spread *F* studies, *Radio Sci.*, *14*, 1111, 1979.

Tsunoda, R.T., R.C. Livingston, J. J. Buonocore, and A.V. McKinley, The frequency-agile radar: a multi-functional approach to remote sensing of the ionosphere, submitted to *Radio Sci.*, 1994.

Whitehead, J.D., Ionization disturbances caused by gravity waves in the presence of an electrostatic field and a background wind, *J. Geophys. Res.*, *76*, 238, 1971.

Woodman, R.F., and C. LaHoz, Radar observations of *F*-region equatorial irregularities, *J. Geophys. Res.*, *81*, 5447, 1976.

Yamamoto, M., S. Fukao, R.F. Woodman, T. Ogawa, T. Tsuda, and S. Kato, Midlatitude *E* region field-aligned irregularities observed with the MU radar, *J. Geophys. Res.*, *96*, 15,943, 1991.

Zalesak, S.T., S.L. Ossakow, and P.K. Chaturvedi, Nonlinear equatorial spread *F*: The effect of neutral winds and background Pedersen conductivity, *J. Geophys. Res.*, *87*, 151, 1982.